# Higher Order Modes as Accuracy Limiting Factor in Permittivity Measurements of High Lossy Fluids Using Transmission Techniques in the GHz Range

A. Redhardt, H.-J. Steinhoff, J. Schlitter, H.-J. Neumann, and G. Hess
Institut für Biophysik der Ruhr-Universität Bochum

Z. Naturforsch. **44a**, 75–80 (1989); received October 12, 1988

The higher order mode distortion in measuring dielectric constants on high lossy, high permittivity liquids in the GHz range is investigated by a simulation procedure as well as by experiment. For this, a homodyne method for measuring $\varepsilon^*$ is introduced in analogy to precision EPR-work.

## 1. Introduction

The complex dielectric constant $\varepsilon^*$ of water was measured by Pottel, Giese, Kaatze, and Uhlendorf [1, 2] in the frequency range from 1.8 to 58 GHz using interferometric methods. A spread around 1% in the values of the complex permittivity of water at 25 °C was reported. As Kaatze and Giese [3] mentioned, higher accuracies up to 0.1% should be possible at the cost of instrumental versatility. A critical point here seems to be the generation of unwanted higher order modes in the transmission line systems [4] used successfully in the broad band experiments cited.

Using a transmission line system, Krüger, Schollmeyer, and Barthel [5] have shown that the accuracy in measuring the attenuation constant of high lossy liquids using this system is limited by the generation of higher order modes in the measuring cell. In a monograph by Grant, Sheppard, and South [6] it was concluded that good separation of the higher modes in waveguides, filled with high lossy, high permittivity liquids cannot be achieved.

Now, in recent papers [7, 8] the complex dielectric constant $\varepsilon^*$ of water and aqueous solutions at 9 GHz was given with an accuracy in the range 0.5–1.5‰. This is to be compared with the results above, especially with the physical argumentation of Krüger, Schollmeyer, and Barthel [5].

We therefore think that this limiting problem of higher modes has to be reinvestigated under a physical point of view using modern techniques if the promille accuracy should be reached practically in physical, chemical and biological measurements. Therefore we present here a numerical method first, which is suitable to simulate the higher mode distortions and to calculate the $\varepsilon^*$-errors. Using this method, it was possible also to calculate a typical distorted field distribution from the experiment.

This method is checked by a homodyne system, as it is used in high precision EPR work but new for $\varepsilon^*$-measurements.

Reprint requests to Prof. Dr. A. Redhardt, Institut für Biophysik, Universität Bochum, Universitätsstraße 150, Postfach 10 21 48, D-4630 Bochum 1.

## 2. The Homodyne System

Figure 1 sketches the principle of the experiment. A klystron feeds power into a waveguide which is filled with the aqueous solution under test. A movable probe senses the local field strength and delivers a signal voltage $U_S$ at the crystal diode D. The phase and amplitude of $U_S$ depend on the probe position $Z$. A constant reference voltage $U_R$ is added to the signal voltage $U_S$ at the diode (cf. Fig. 1), $|U_R + U_S|$ causing lastly a dc-output $V_{tot}(Z)$ which depends on the probe position $Z$.

From this dependency, $\varepsilon^*$ of the liquid as well as the higher mode field distribution are calculated.

To complete the analogy to precision EPR-work, we suppose

$$|U_R| \gg |U_S|. \tag{1}$$

The combination of the sketched homodyne principle with (1) allows simple $\varepsilon^*$-determinations with high accuracy. In EPR-work, this combination allows the precise determination of spin concentrations [9].

Now, we assume:

(i) The diode input partial VHF-voltage $\Delta U$, which changes when changing $Z$, is $\Delta U \equiv |U_R + U_S|$

0932-0784 / 89 / 0100-0075 $ 01.30/0. – Please order a reprint rather than making your own copy.

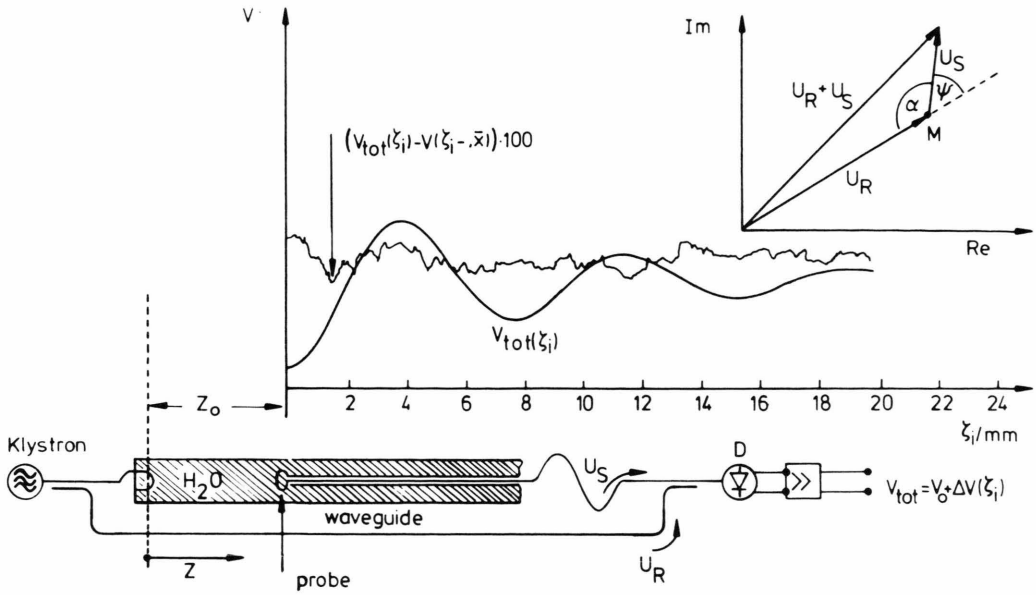


Fig. 1. Bottom: Schematic diagram for measuring $\varepsilon^*$ by transmission technique, using a highly biased diode. Middle: Registration of wave transmission in water in the waveguide R 500 together with computed difference plot. Insert: Vector-addition of signal voltage $U_S$ and biasing reference voltage $U_R$ at the diode.

$-|U_R| \approx U_S \cos\psi$ (cf. Figure 1). The better (1) is fulfilled, the better holds (i).

(ii) The systems dc-output partial voltage $\Delta V(Z)$ is proportional to $\Delta U$ (cf. Figure 1).

(iii) The wave, reaching the probe in the waveguide, is the fundamental mode only. This is the problem to be discussed in this paper.

The probe starts its movement at the position $Z_0$. It is set at $Z = Z_0 + \zeta$ with $\zeta$ as running coordinate. Now, at discrete valus $\zeta_i$ ($i = 1, \ldots, N = 1024$) the total dc-output voltage $V_{tot}(\zeta_i)$ of the system is stored in a computer and handled further.

If the assumptions (i)–(iii) hold, then $V_{tot}(\zeta_i) = V_0 + \Delta V(\zeta_i)$ should be representable by

$$V(\zeta_i; X) = V_0 + V \sin(\varkappa' \zeta_i) + \psi_0) \exp(-\varkappa'' \zeta_i). \tag{2}$$

Equation (2) contains 5 adjustable parameters ($V_0$, $V$, $\varkappa'$, $\varkappa''$, $\psi_0$), designated as parameter vector $X$. Now, we start with an approximate parameter vector, the components of which are, e.g., graphically taken from an experiment like Figure 1. Then the starting error square sum $Q$

$$Q(X) = \sum_{i=1}^{N} [V_{tot}(\zeta_i) - V(\zeta_i, X)]^2 \tag{3}$$

is calculated. Hereafter $Q(X)$ is minimized by varying $X$, using known procedures [10]. As final result of this minimizing procedure (which takes with 6 iterations on a Cyber 855 about 18 sec CPU-time) we get an optimum parameter vector $\bar{X} = (\bar{V}_0, \bar{V}, \bar{\varkappa}', \bar{\varkappa}'', \bar{\psi}_0)$. Now, we are interested only in $\bar{\varkappa}'$ and $\bar{\varkappa}''$. These quantities we identify with the propagation constant $\bar{\varkappa}^* = \bar{\varkappa}' - j\bar{\varkappa}''$ of the fundamental mode in the liquid filled waveguide. Then the complex dielectric constant $\varepsilon^* = \varepsilon' - j\varepsilon''$ of the liquid is given by

$$\begin{aligned} \varepsilon' &= \frac{\bar{\varkappa}'^2 - \bar{\varkappa}''^2 + \bar{\varkappa}_c^2}{\varkappa_0^2}, \qquad \varkappa_0^2 = \omega^2 \varepsilon_0 \mu_0, \\ \varepsilon'' &= \frac{2\bar{\varkappa}'\bar{\varkappa}''}{\varkappa_0} - \frac{\sigma}{\varepsilon_0 \omega}, \qquad \varkappa_c = \frac{2\pi}{\lambda_c}, \end{aligned} \tag{4}$$

where the symbols on the right have their usual meaning.

## 3. Higher Modes: The Numerical Check Procedures

Equation (3) can be used as overall check of the measuring system as well as to investigate error influences by numerical simulation of these errors. We sketch both procedures.

*(a) Overall Check*

Equation (4) holds only, if (2) describes the field distribution correctly. To check this, we draw a difference plot

$$f(\zeta_i; \bar{X}) = [V_{\text{tot}}(\zeta_i) - V(\zeta_i; \bar{X})] \cdot 100. \tag{5}$$

Then the plot of $f(\zeta_i; \bar{X})$ must not show any periodicity. Figure 1 gives examples for both $V_{\text{tot}}(\zeta_i)$ and $f(\zeta_i, \bar{X}) \cdot 100$.

*(b) Error Simulation*

Our error simulation was developed primarily to investigate the higher mode problem. However, it can be used to study many other error sources in this context, as will be shown. Therefore we discuss the procedure on a special example of the higher mode problem in detail. There are three steps necessary:

(i) First, we calculate the function $V(\zeta_i, V_0, V, \varkappa', \varkappa'', \psi_0)$, (2), in the range $i = 1, \ldots, 1024$. For this, $\varkappa'$ and $\varkappa''$ are calculated for the fundamental mode $TE_{10}$ in the waterfilled waveguide R 500 from literature values; $V_0$, $V$, and $\psi_0$ are choosen arbitrarily.

(ii) Now, the function calculated in (i) is modified so as to simulate the error to be investigated. In our case, this modification includes additional wave (higher mode simulation) additively, which are calculated using $\varkappa'$ and $\varkappa''$ from (i). We denote this modified function by $V_M(\zeta_i)$.

(iii) The error square sum

$$Q = \sum_{i=1}^{N} [V_M(\zeta_i) - V(\zeta_i; X)]^2 \tag{6}$$

is calculated and minimized by varying the parameter vector $X$ as described. The parameter vector which minimizes $Q$ is called $\bar{X}$ again; $\bar{X} = (\bar{V}_0, \bar{V}, \bar{\varkappa}', \bar{\varkappa}'', \bar{\psi}_0)$. The complex propagation constant $\bar{\varkappa}^* = \bar{\varkappa}' - j\bar{\varkappa}''$ describes best the distortion field distribution $V_M(\zeta_i)$. Clearly, $\bar{\varkappa}^*$ is different from the true $\varkappa^*$ we had used to construct $V_M(\zeta_i)$.

Then, using (4) and putting there $\bar{\varepsilon}^*$ instead of $\varepsilon^*$ we calculate the relative errors

$$\frac{\Delta\varepsilon'}{\varepsilon'} = \frac{\varepsilon' - \bar{\varepsilon}'}{\varepsilon'}; \quad \frac{\Delta\varepsilon''}{\varepsilon''} = \frac{\varepsilon'' - \bar{\varepsilon}''}{\varepsilon''} \tag{7}$$

which are the higher mode errors resulting from the field distortion assumed.

*(c) Higher Mode Errors: The Error Simulation Scheme*

Firstly we choose for $V_M(\zeta_i)$ a function which consists of the principal mode $TE_{10}$ and one distorting mode denoted by the index $q$:

$$V_M(\zeta_i) = V_0 + V_1(Z_0) \sin(\varkappa_1' \zeta_i + \psi_1) \exp(-\varkappa_1'' \zeta_i) + V_q(Z_0) \sin(\varkappa_q' \zeta_i + \psi_q) \exp(-\varkappa_q'' \zeta_i). \tag{8}$$

In this expression we first calculate $\varkappa_1'$ and $\varkappa_1''$, using the inverted Eq. (4) with values of $\varepsilon^*_{H_2O}$ taken here from [11]. Now $\varkappa_q^*$ can be calculated because it is connected to $\varkappa_1^*$ by

$$\left.\begin{matrix}\varkappa_q' \\ \varkappa_q''\end{matrix}\right\} = \left\{\frac{[(\varkappa_1'^2 - \varkappa_1''^2 + \varkappa_{c1}^2 - \varkappa_{cq}^2)^2 + (2\varkappa_1'\varkappa_1'')^2]^{1/2} \pm [\varkappa_1'^2 - \varkappa_1''^2 + \varkappa_{c1}^2 - \varkappa_{cq}^2]}{2}\right\}^{1/2}. \tag{9}$$

$V_0$, $V_1(Z_0)$, $\psi_1$ and $\psi_q$ can be choosen arbitrarily.

The same holds for $V_q(Z_0)$. However, the quantity $V_q(Z_0)/V_1(Z_0) \equiv \eta$ has the physical meaning of the strength of the higher mode (index q) at $Z_0$ relativ to the strength of the fundamental mode (index 1) at $Z_0$. Now, the error square sum (6) is minimized with $V_M(\zeta_i)$ from (8), and the resulting errors $\Delta\varepsilon'/\varepsilon'$ and $\Delta\varepsilon''/\varepsilon''$ are calculated as described. Physically, this procedure describes a situation where a higher mode q is present, but the computer calculates $\varepsilon^*$ with the assumption that only the fundamental mode is present.

In this case, we find periodicity in the difference plot, if $\eta > 10^{-3} \ldots 10^{-2}$.

## Higher Modes, Results

As the calculations show, the errors in $\varepsilon^*$ are nearly proportional to the contamination constant $\eta$ in the range $\eta = 0.5 \ldots 10^{-3}$.

In this range

$$\frac{\Delta\varepsilon'}{\varepsilon'} = F'\eta, \quad \frac{\Delta\varepsilon''}{\varepsilon''} = F''\eta, \tag{10}$$

the constants $F'$, $F''$ depending on the propagation mode, waveguide type and frequency. Table 1 summarizes some results for the waveguides R 500 and R 320 used here, as well as for an oversized waveguide WR 102 [8].

We see that accuracies in the promille range correspond roughly to $\eta = 10^{-3} \ldots 10^{-2}$.

Table 1. The figures in the table give the "distortion powers" $F'$ and $F''$ of the respective modes, following from (10), in water filled waveguides. As can be seen, in the oversized waveguide WR 102 the distortion power $F'$ of $TE_{30}$ is larger than in R 500. Additionally, a comparison with Table 2 shows very similar $\varkappa''$-values for $TE_{30}$ and $TE_{10}$ in WR 102 used in [8]. In R 500 used here, the distortion power $F'$ of $TE_{30}$ is smaller; additionally the $\varkappa''$ of $TE_{30}$ is according to Table 2 considerably larger then the $\varkappa''$ of the fundamental $TE_{10}$, allowing for effective mode separation.

| Waveguide | R 500 (8.35 GHz) | | R 320 (3.5 GHz) | | WR 102 (8.35 GHz) | |
|---|---|---|---|---|---|---|
| Fundamental mode $TE_{10}$ + distortion mode | $TE_{30}$ | $TE_{01}$ | $TE_{30}$ | $TE_{01}$ | $TE_{30}$ | $TE_{01}$ |
| $F'$ | 0.030 | 0.202 | 0.0027 | 0.0088 | 0.046 | 0.016 |
| $F''$ | 0.093 | 0.491 | 0.0039 | 0.0435 | 0.011 | 0.0015 |

Table 2. The attenuation constant $\varkappa''$ for water at 298 K with different waveguides and frequencies. $\varkappa''_{TE_{10}}$-values are given at the head of each column. The other figures give relative values $\varkappa''_{TE_{mn}}/\varkappa''_{TE_{10}}$. In the smaller waveguides the ratios are $\gg 1$, increasing with mode order and enabling mode separation. For the oversized WR 102 [8], the similarity of $\varkappa''$ of these modes makes mode separation impossible.

| | | | 8.35 | 9.35 | 11.35 GHz 298 K |
|---|---|---|---|---|---|
| R 500 | $m$ | $n$ | $\varkappa''_{10/mm^{-1}} = 0.309$ | $=0.369$ | $=0.499$ |
| 4.78 | 0 | 1 | 1.707 | 1.457 | 1.254 |
| $\cdot 2.39\ mm^2$ | 0 | 2 | 7.169 | 5.762 | 3.819 |
| | 1 | 0 | 1 | 1 | 1 |
| | 1 | 1 | 2.223 | 1.744 | 1.380 |
| | 1 | 2 | 7.476 | 6.028 | 4.099 |
| | 2 | 0 | 1.708 | 1.458 | 1.254 |
| | 2 | 1 | 4.003 | 3.015 | 1.946 |
| | 2 | 2 | 8.330 | 6.766 | 4.673 |
| | 3 | 0 | 4.507 | 3.444 | 2.193 |
| | 3 | 1 | 6.163 | 4.887 | 3.215 |
| | 3 | 2 | 9.587 | 7.846 | 5.509 |
| R 620 | $m$ | $n$ | $\varkappa''_{10/mm^{-1}} = 0.335$ | $=0.392$ | $=0.520$ |
| 3.75 | 0 | 1 | 2.88 | 2.183 | 1.552 |
| $\cdot 1.88\ mm^2$ | 0 | 2 | 9.030 | 7.543 | 5.412 |
| | 1 | 0 | 1 | 1 | 1 |
| | 1 | 1 | 3.729 | 2.865 | 1.884 |
| | 1 | 2 | 9.368 | 7.829 | 5.643 |
| | 2 | 0 | 2.885 | 2.185 | 1.553 |
| | 2 | 1 | 5.661 | 4.571 | 3.067 |
| | 2 | 2 | 10.315 | 8.652 | 6.288 |
| | 3 | 0 | 6.182 | 5.033 | 3.430 |
| | 3 | 1 | 7.935 | 6.578 | 4.656 |
| | 3 | 2 | 11.725 | 9.874 | 7.238 |
| R 740 | $m$ | $n$ | $\varkappa''_{10/mm^{-1}} = 0.376$ | $=0.427$ | $=0.549$ |
| 3.09 | 0 | 1 | 3.897 | 3.148 | 2.111 |
| $\cdot 1.55\ mm^2$ | 0 | 2 | 10.088 | 8.753 | 6.608 |
| | 1 | 0 | 1 | 1 | 1 |
| | 1 | 1 | 4.719 | 3.902 | 2.672 |
| | 1 | 2 | 10.441 | 9.068 | 6.860 |
| | 2 | 0 | 3.899 | 3.151 | 2.113 |
| | 2 | 1 | 6.623 | 5.640 | 4.085 |
| | 2 | 2 | 11.436 | 9.954 | 7.568 |
| | 3 | 0 | 7.150 | 6.116 | 4.475 |
| | 3 | 1 | 8.948 | 7.733 | 5.788 |
| | 3 | 2 | 12.925 | 11.278 | 8.621 |
| WR 102 | $m$ | $n$ | $\varkappa''_{10/mm^{-1}} = 0.278$ | $=0.339$ | $=0.471$ |
| 12.9 | 0 | 1 | 1.010 | 1.008 | 1.006 |
| $\cdot 25.6\ mm^2$ | 0 | 2 | 1.055 | 1.044 | 1.030 |
| | 1 | 0 | 1 | 1 | 1 |
| | 1 | 1 | 1.014 | 1.011 | 1.008 |
| | 1 | 2 | 1.059 | 1.047 | 1.032 |
| | 2 | 0 | 1.010 | 1.008 | 1.006 |
| | 2 | 1 | 1.025 | 1.020 | 1.014 |
| | 2 | 2 | 1.071 | 1.056 | 1.039 |
| | 3 | 0 | 1.028 | 1.023 | 1.016 |
| | 3 | 1 | 1.043 | 1.035 | 1.024 |
| | 3 | 2 | 1.092 | 1.073 | 1.050 |

To reach small $\eta$-values, a carefully matched coupling system (window [12], loop) must be used first. Additionally, Table 2 shows a strong dependency of $\varkappa''$ on mode, waveguide type, and frequency. Here, the dependency of $\varkappa''$ on the mode inceases if the ratio wavelength/waveguide dimensions increases, as it is to be expected from field theory.

Hereafter, a "natural", effective mode separation by different $\varkappa''$ is possible also for high lossy, high permittivity liquids. This result is in contradiction to [6]. Beyond that, it seems to be of importance for new high precision $\varepsilon^*$ measurements on these liquids.

It should be stressed that Kaatze [12] reported an accuracy level of 1% in measuring $\varepsilon^*$ also with oversized waveguides. We conclude that mode separation can be reached in two ways: By careful excitation conditions as well as by choosing suitable small waveguide dimensions. Both possibilities should be used in the promille accuracy range.

## Experimental Determination of Higher Order Modes

For a lossless, coaxial line system beyond cutoff at low frequencies, in [13] the field distribution around a discontinuity of the inner conductor was calculated. It was shown that a large number of higher modes in comparable intensity is necessary to fulfill the boundary conditions.

Now, in a lossy medium, the $TE_{mn}$-waves, as well as the $TM_{mn}$-waves are not an orthogonal system as in lossless electromagnetic waveguides. Therefore a rigorous solution of the problem should be difficult.

If, however, in our case $Z_0$ is large enough, instead of (2), a sum of $TE_{mn}$ waves should be a good description of the real field distribution. We discuss this sum qualitatively first. Here, the modes $TE_{mn}$: $m = 0, 2, 4, 6$; $n > 1$ can be supressed by symmetric excitation. Therefore the next odd mode $TE_{30}$ should mainly contribute to the field at small $Z_0$-values.

After this, we are now describing a real experiment at small $Z_0$-values. Following the arguments given above, we try instead of (2) a function

$$V(\zeta_i) = V_0 + V_{10}(Z_0)\sin(\varkappa'_{10}\zeta_i + \psi_{10})\exp(-\varkappa''_{10}\zeta_i) + V_{30}(Z_0)\sin(\varkappa'_{30}\zeta_i + \psi_{30})\exp(-\varkappa''_{30}\zeta_i). \tag{11}$$

*Since* (9) connects $\varkappa^*_{10}$ and $\varkappa^*_{30}$, there remain seven independent fit parameters: $V_0$; $V_{10}(Z_0)$, $\varkappa'_{10}$, $\psi_{10}$, $\varkappa''_{10}$, $V_{30}(Z_0)$ and $\psi_{30}$, which have to be determined from the experiment as described above. If (11) indeed describes the experimental higher order mode distortion, then three conditions must hold simultaneously. They are:

(i) $V_{10}(Z_0)$ must depend exponentially on $Z_0$: $\ln V_{10}(Z_0) = a_1 - \varkappa''_1 Z_0$.
(ii) Similarly, $\ln V_{30}(Z_0) = a_3 - \varkappa''_3 Z_0$ must hold.
(iii) The quantities $\varkappa''_1$ and $\varkappa''_3$ taken from these plots must be identical with the literature values $\varkappa''_{10}$ and $\varkappa''_{30}$ of the attenuation constants for the liquid investigated in the waveguide used ($H_2O$ in R 500).

Figure 2 shows that (i)–(iii) are well fulfilled indeed, confirming our method and assumptions.

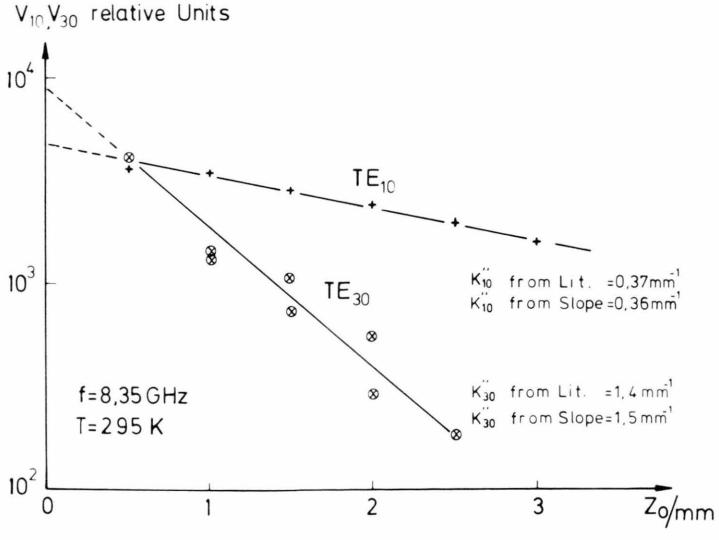


Fig. 2. Experimental field analysis near the coupling loop measured in water filled R 500. Ordinate: $V_{10}(Z_0)$; $V_{30}(Z_0)$ after (11). The distortion of the fundamental mode $TE_{10}$ is dominated by $TE_{30}$. Both modes have at $Z_0 = 0$ (incoupling) comparable field intensities.

This experiment, together with the attenuation constants, Table 2, gives us as a practical lower bound $Z_0 > 10$–$15$ mm for $TE_{30}$ amplitudes relative to $TE_{10}$ being smaller than $10^{-4}$ (water R 500, 10 GHz, 298 K) higher modes having considerably higher attenuation constants in the waveguide used.

## Summary

The higher mode distortions in measuring $\varepsilon^*$ in high lossy, high permittivity liquids ar calculated by a simulation method and investigated experimentally. They can be made negligibly small. Hereafter, it should be possible to perform high precision absolute measurements of $\varepsilon^*$ on these liquids with medium sized waveguides. A homodyne type method for this is proposed.

*Acknowledgement*

We thank Prof. R. Pottel for helpful discussions, Mr. K. Lieutenant and Mr. O. Dombrowsky for numerical calculations, Mr. Chr. Bassaris for the drawings and Mrs. H. Schlegel for typewriting the manuscript.

[1] R. Pottel, K. Giese, and U. Kaatze, Structure of Water and Aqueous Solutions, Ed. W. A. P. Luck, Verlag Chemie, Weinheim 1974.
[2] U. Kaatze and V. Uhlendorf, Z. Phys. Chemie N.F. **126,** 151 (1981).
[3] U. Kaatze and K. Giese, J. Phys. E. Sci. Instrum. **13,** 133 (1980).
[4] T. J. Buchanan and E. H. Grant, Brit. J. Appl. Phys. **6,** 64 (1955).
[5] J. Krüger, E. Schollmeyer, and J. Barthel, Z. Naturforsch. A **30,** 1476 (1975).
[6] E. H. Grant, R. J. Sheppard, and G. P. South, Dielectric Behaviour of Biological Molecules in Solution, Clarendon, London 1978.
[7] J. G. McAvoy and H. A. Buckmaster, J. Phys. D. Appl. Phys. **18,** 2109 (1985).
[8] J. G. McAvoy and H. A. Buckmaster, J. Phys. E. Sci. Instrum. **18,** 244 (1985).
[9] A. Redhardt and W. Daseler, J. Biochem. Biophys. Methods **15,** 71 (1987).
[10] D. Braess, Computing **1,** 264 (1966).
[11] U. Kaatze and V. Uhlendorf, Z. Phys. Chem. N.F. **126,** 151 (1981).
[12] U. Kaatze, Adv. Molec. Relax. Processes **7,** 71 (1975).
[13] A. Redhardt, Arch. Elektr. Übertr. **11,** 227 (1957).